Proceedings World Geothermal Congress 2010
Bali, Indonesia, 25-29 April 2010

The Brittle Ductile Transition in Experimentally Deformed Basalt Under Oceanic Crust Conditions: Evidence for Presence of Permeable Reservoirs at Supercritical Temperatures and Pressures in the Icelandic Crust

Violay, M.[1], Gibert, B. [1], Mainprice, D. [1] Evans, B.[2], Pezard, P.A. [1], Flovenz, O.G.[3], Asmundsson, R.[4]

1 Géosciences Montpellier UMR 5243 - CC 60, Université Montpellier 2, Place E. Bataillon, 34095 Montpellier cedex 5; France. Email: marie.violay@gm.univ-montp2.fr

2 Dept. of Earth, Atmospheric, and Planetary Sciences Massachusetts Institute of Technology 77 Massachusetts Ave. Cambridge, MA 02139-4307. USA

3 ISOR, Iceland GeoSurvey, Grensasvegur 9, 108, Reykjavik, Iceland

4 ISOR, Iceland Geosurvey, Rangarvöllum, Akureyri, 603, Iceland

Keywords: Basalt, experimental deformation, Iceland, supercritical fluids.

ABSTRACT

Mechanical properties of rocks at depth control the transport behavior of very high temperature hydrothermal reservoirs. In particular, the brittle to ductile transition in rocks may strongly influence their permeability and the maximum depth and temperature where hydrothermal fluids may circulate. In order to characterize these properties in the context of Icelandic crust, we conducted triaxial compression experiments to investigate the effects of pressure, temperature and strain rate on the rheology of basaltic rocks. The tests were carried out at temperature from 400 to 950°C, confining pressure (P_{conf}) from 100 to 300 MPa, pore pressure (P_p) from 0 to 50 MPa and strain rate ($\dot{\varepsilon}$) from 10^{-6} to 10×10^{-4} s^{-1}. Mechanical and micro-structural observations at a constant strain rate of 1×10^{-5} s^{-1} and a confining pressure of 100 MPa and 300 MPa indicate that the rocks are brittle and dilatant up to 700 to 800°C. At higher temperatures and effective pressures the deformation mode becomes ductile, in the sense that the deformation is less-localized and that no shear rupture plane develops. No single constitutive law is accepted as definitive of the mechanical behavior of rocks within the semi-brittle regime, but if one assumes that the mechanical behavior can be characterized as Mohr-Coulomb in the brittle field and as a steady-state, power law in the ductile field, then the strength at geological strain rates can be estimated. Such an extrapolation suggests that the brittle to ductile transition will strongly depends on the nature of starting material. Glassy basalts may undergo the transition at about 200°C, whereas the same transition might occur in non-glassy basalts at deeper conditions, i.e., temperatures higher than 600-700°C. The effect of the transition on the permeability of basaltic rocks has not been measured, but the brittle-ductile transition might be considered a limit for the depth at which supercritical hydrothermal fluids may circulate. For basaltic crust with a geotherm similar to that under Iceland, an estimate of depth of the brittle-ductile transition is about 6 to 8 km, results that are consistent with the lower limit of the Icelandic seismogenic zone which seems to be associated with a 750 ± 100 °C isothermal surface.

1. INTRODUCTION

The mid-ocean ridge system is the largest continuous volcanic feature on Earth, with significant interactions between tectonic activity, volcanism and sea-water circulation *(Macdonald, 1982).* Iceland is the largest landmass straddling a mid-ocean ridge. The associated tectonic and volcanic settings resulting from the active rifting provide, in this geodynamic context, a major heat source for the geothermal exploitation *(Pálmason and Sæmundsson, 1979).* In this context, supercritical fluids are of great interest for geothermal energy as their extraction may enhance by a factor of ten the electrical power of conventional geothermal power plants *(Albertsson et al., 2003).* Producing supercritical fluids will require the drilling of wells and sampling of fluids and rocks at depths of 3.5-6 km, and at temperatures between 450 and 700°C *(Fridleifsson, 2005).* Our study is part of the so called HITI project (HIgh Temperature Instruments for supercritical geothermal reservoir characterization and exploitation - funded by the European Union) and IDDP (Iceland Deep Drilling Project) whose main objective is to characterize the physical properties of the deep reservoir in order to produce supercritical hydrous fluids from drillable depths *(Fridleifsson, 2005; Massiot et al., 2009 in prep).* One very important parameter influencing the permeability of very high temperature reservoirs is inelastic deformation. In particular, the brittle to ductile transition in rocks has often been regarded as indicating the maximum depth and temperature at which hydrothermal fluids may circulate.

2. METHODS AND SAMPLES

Deformation experiments were conducted in a triaxial servo-controlled internally gas medium apparatus from "Paterson Instruments" at temperatures of 400°C to 900°C, lithostatic confining pressures (P_c) varying from 100 MPa to 300 MPa, and pore pressures (P_p) from 0 to 50 MPa. Deformation experiments were performed at constant strain rates ($\dot{\varepsilon}$) where $10^{-6}\ s^{-1} \leq \dot{\varepsilon} \leq 10^{-4}\ s^{-1}$, up to strains of 15%. Argon was used as confining medium as well as pore fluid. Strain rate and pore pressure have been changed in a few exploratory runs in order to investigate their effects on differential stress. Differential stress was measured with an accuracy of 2 MPa (Fig. 1).

Cylindrical samples of 10 mm in diameter and 20 mm in length were jacketed with copper or iron. Copper was used to reduce the effect of jacket strength on mechanical data at low temperature (400 to 700°C) whereas iron was used at higher temperature. After deformation, samples were impregnated with glue, cut perpendicular to the shear zone, and thin sections were prepared to observe microstructures.

Two different types of basalts were selected for their simple compositions low degree of alteration, and very low porosity (<2%). The rocks differed in their percentage of glass, being zero in one case and about 15% in the other.

The glassy basalt (*GB*) is composed of roughly 10 by vol.% phenocrysts (olivine, clinopyroxene, and plagioclase) and 90% of a cryptocrystalline groundmass. The groundmass contains evenly distributed fines of 60-65% plagioclase; 10-15% clinopyroxene, 2-3% oxide, and 10-15% glass. The second sample source was microcrystalline glass-free basalt (*GFB*) composed of 5 by vol.% phenocrysts (olivine, clinopyroxene, and plagioclase) and 95% of a finer-grained groundmass. The groundmass contains homogeneously distributed 65-70% plagioclase, 15-20% clinopyroxene, and 5-10% oxide.

3. RESULTS

The results of 16 triaxial deformation tests are illustrated in Figure 1.

3.1 Mechanical Data

3.1.1 *GB* Sample

For the vitreous sample *GB*, elastic deformation at low strain (<2%) is followed by three–deformation modes depending on temperature and pressure (Fig.1):

(1) At 400°C and confining pressure of 100 MPa, brittle fracturing with a maximum stress of 900 MPa occurs, corresponding to failure by localized rupture, often along two conjugate zones, creating a wedge of material near the end of the sample.

(2) Between 500°C to 700°C with a confining pressure of 100 MPa, the sample fails by localized rupture, typically along a single zone, with a yield stress of 180 MPa which is independent of temperature. The rock strain hardens at small strains, until the ultimate strength is reached, after which, sliding on a localized fracture plane occurs at roughly constant stress. At lower effective pressures (increasing pore pressure), peak strength is followed by strain weakening and stress stabilization at higher strain (about 5%).

(3) At temperature from 800 to 900°C with confining pressure of 100 MPa, and from 600°C to 900°C with confining pressure of 300 MPa, the samples show distributed semi-brittle to ductile flow is experienced at differential stresses from 50 to 100. At these temperatures maximum sample strengths showed high temperature dependence but very low pressure dependence.

3.1.2 *GFB* Sample

For the glass-free sample (*GFB*), elastic deformation at low strain (<2%) is followed by two deformation modes depending on temperature and pressure (Fig. 1):

(1) At a confining pressure of 100 MPa and between 600°C and 900°C and at 300 MPa between 600°C and 800°C, the sample fails by localized rupture with a peak strength that depends on temperature and pressure. The peak strength increases as temperature decreases and pressure increases. In experiments where rupture is not accompanied with gas leakage, peak stress is systematically followed by strain weakening, and by a stabilization of differential stress at strains of about 5-10%. As is common in other brittle rocks, this is the result of localized deformation and sliding on a shear plane *(e.g. Escartin et al¸2008).*

(2) With increasing temperature up to 800°C and 950°C at 300 MPa the samples undergo a transition from strain weakening to moderate strain hardening. Strain hardening was observed in experiments conducted at 800 to 950°C at 300 MPa and corresponds to homogeneous and distributed ductile flow.

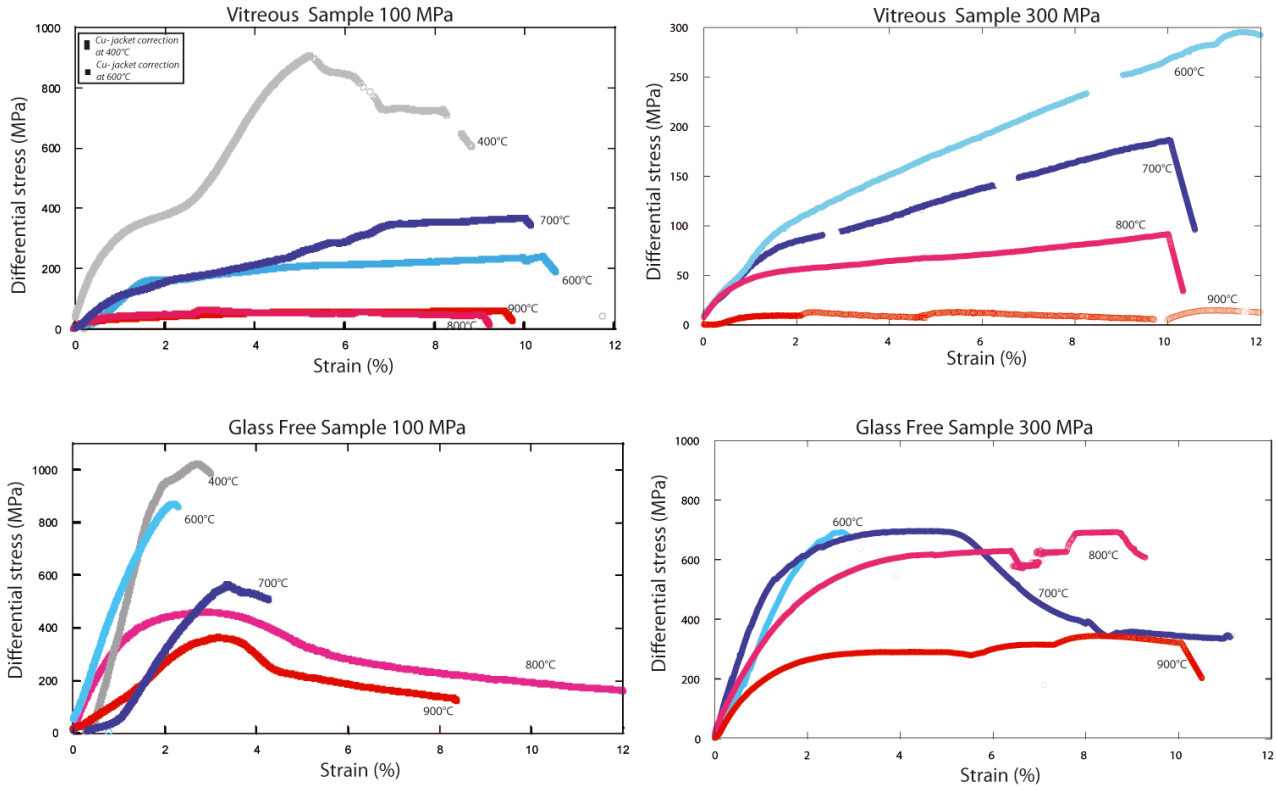

Figure 1: Differential stress versus strain curves for experiments conducted at temperature between 400 and 900°C and confining pressure P_{conf} from 100 to 300 MPa. The initial strain rate for all experiments was 10^{-5} s^{-1}.

3.2 Micro-Structural Observations

The micro-structures of deformed samples were observed using the scanning electron microscope (SEM) and optical microscope (Fig. 2).

3.2.1 *GB* Sample

At 400°C and 100 MPa, *GB* failed by wedge splitting. *GB* sample in the range of 500 to 700°C failed by brittle fracturing associated with the formation of a localized shear fracture. Shear zones are oriented between 30° and 40° to compression direction. Their thickness increase when the effective pressure decreases and when temperature increases, from 10 µm to 50 µm. Fault zones imaged in SEM with back-scattered electron (BSE) contrast contain angular fragments that range from 0.01 µm to 10 µm. The fault zone changed orientation near the phenocryst boundary (Fig. 2).

In the temperature range of 800 to 900°C at 100 MPa and 600°C to 900°C at 300 MPa the samples do not display localized deformation. The glass volume fraction has been reduced.

3.2.2 *GFB* Sample

At 400 to 700°C *GFB* failed by wedge splitting. In the range of 800 to 900° at 100 MPa and 600 to 700°C at 300 MPa sample *GFB* failed by brittle fracture accompanied with the formation of localized shear fractures arranged en echelon. They are oriented between 30° to 45° to the compression direction. SEM-BSE images show that the fault zones contain angular fragment that range from 0.01 µm to 10 µm. At 800°C to 900°C deformation is distributed in spite of plagioclase crystals having strong preferential orientation around the phenocrysts.

4. DISCUSSION

Combination of mechanical and micro-structural data indicates that a transition from brittle to ductile behaviour is observed in the investigated temperature and pressure range, at a strain rate of 10^{-5} s^{-1}. This transition strongly depends on the nature of starting material, glassy basalt showing ductile behaviour at lower P, T conditions than glass free basalts. In order to quantify both brittle and ductile deformation regimes, stress-strain curves were interpreted in terms of friction laws and steady-state power law creep. However, given the complexity of the mechanical behavior of our samples, it is necessary to make some qualifications.

In fact, the exact departure from strictly linear behavior is often not clear, and therefore it is difficult to define precise yield points. A further complication is that the initial slope of the stress-strain curves varies from one set of conditions to another, the initial slopes of the curves are typically more compliant with increasing temperature and decreasing pressure. The clearest trend of the post-yield behavior is the effect of temperature: the peak strength for both the glassy and glass-free basalts depends indirectly on temperature. Both sets of rocks also depend on deformation rate, as would be expected for temperature-activated deformation. The pressure-dependence of strength is more ambiguous. For glass-free basalts, with the exception of the data at 600°C, increasing the effective lithostatic pressure increases the peak strength. For the glass-free rocks, load drops are delayed to larger strains or are entirely absent when the effective pressure is increased. For the vitreous samples, the strengths are larger at lower pressures, corresponding to an unusual behavior for rocks deforming by cataclastic processes. One extremely important parameter in cataclastic deformation under confined conditions is the pressure of any pore fluids that are present. Our experiments were nominally drained, but we did not attempt to directly monitor the fluid pressure within the pore space of the rock. If the samples are subject to the normal restrictions of Mohr-Coulomb behavior at the local scale, then the results suggest that the effective pressure was systematically over-estimated in experiments at higher pressures. Alternatively, it may be that deformation in the more-highly confined rocks was dominated by pressure-independent mechanisms. Further data are needed to discriminate between these possibilities. In both rock types, strength evolves during the experiments, except at the highest temperature, 900°C. Load drops are more prevalent in the glass-free rocks at low pressures, whereas most of the other experiments exhibit strain-hardening, although the hardening rate seems to decrease with increasing temperature. Both the suppression of load drops and strain-hardening behavior are characteristic of rocks deforming in the semi-brittle regime, where local deformation is partitioned between cataclastic and crystal-plastic mechanisms. The experiments performed here were limited to strains below about 15%, and thus, we do not know if load drops or steady-state strength would occur at much higher strain. Also the use of laws of friction and steady-state power law creep can only be used as a first approximation.

4.1 Brittle Behavior

In order to quantify the brittle deformation shown by the mechanical results and micro-structural observations, the friction (sliding) coefficient was determined by using the pressure dependence of differential stress measured once sliding on the shear plane is assumed stable (characterized by a constant value of differential stress). Sliding stress, peaked at 2% of permanent strain after stress drop associated with localization, is plotted versus effective pressure (Fig. 1). Mohr circles are drawn using the maximum differential stress measured at $\dot{\varepsilon} = 10^{-5}s^{-1}$ in each experiment (Fig. 3) with $\sigma_3 = P_{eff.}$ A linear fit between σ_1-σ_3 and P_{eff} gives a slope $\mu' = 1.3$ with a Y intercept which represents the uniaxial compressive strength, of σ_0=106MPa. The coefficient of friction µ and the cohesive strength C are constrained by the equivalence relations *(Paterson, 1978)*, where

$$\tau = C + \mu\sigma_n \quad (1)$$

$$\text{and } \mu=\mu'/(2\sqrt{(1+\mu')}) \text{ ... } C= \sigma 0/(2\sqrt{(1+\mu')}) \quad (2)$$

Using the linear fit approximately tangent to the Mohr circles indicates a coefficient of friction of µ= 0.42 and a cohesive strength of 34 MPa.

Sliding stress is weakly dependent on the temperature between 600 and 700°C and between 800 and 900°C at 100 MPa, in *GB* and *GFB*, respectively. Values of friction coefficient are in agreement with previous studies on various silicate rocks at low temperature ($0.43<\mu<0.6$) *(Rocchi et al., 2003)*.

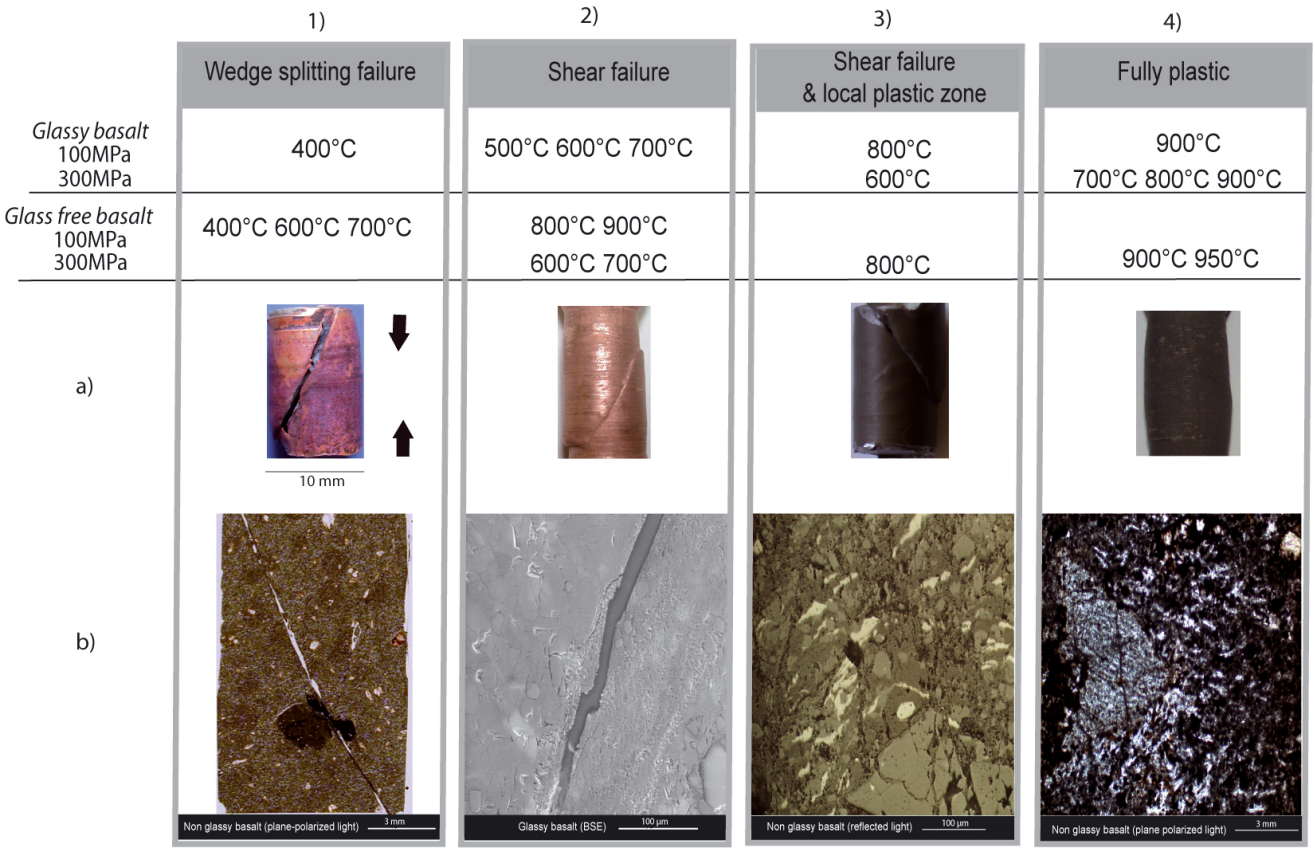

Figure 2: Photographs of jacketed deformed samples and microstructures of several deformed samples of basalt on thin sections. 1) Optical plane-polarized light microphotograph of microstructure of GFB at 400°C P_{conf} 100 MPa shows wedge splitting. 2) Backscattered Scanning Electron microphotograph failed by brittle fracture with the formation of a localized shear fracture. 3) Reflected light microphotograph, sample were deformed in a semi-brittle regime with evidence of localized rupture and several plastic zone. 4) Optical plane-polarized light microphotograph shows distributed deformation under fully plastic mode.

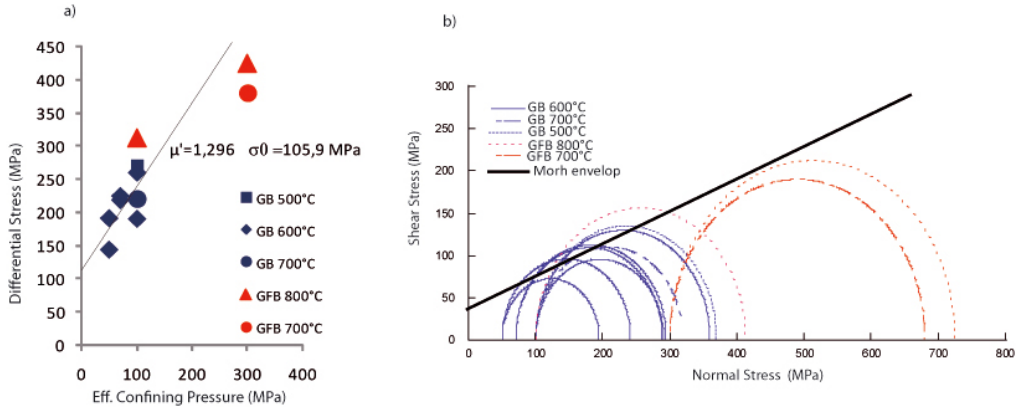

Figure 3: Maximum differential stress variation with effective confining pressure. a) Linear least squares fit to effective confining pressure versus friction stress at strain rate of $10^{-5}s^{-1}$. b) Mohr circle constructed with the data Figure 3a. The line that is approximately tangent to the Mohr circles indicates coefficient μ = 0.42 and C = 34 MPa.

4.2 Semi-Brittle to Ductile Behavior

For all experiments where mechanical and micro-structural observations show evidence of ductile deformation we use the following equation (3) to describe the steady state flow.

In fact, deformation at high temperature and pressure in rocks is often described using a steady-state power law of the form:

$$\varepsilon' = A.\sigma^{n}.\exp((-(Q))/RT) \quad (3)$$

where έ is the axial strain rate, σ the differential stress, A is a material constant, *Q* the activation energy, R the gas constant, and T the absolute temperature. Because of the influence of cataclastic mechanisms (highlighted by strain hardening behaviour at high strain, see above), using a constitutive law of this form will be, at best, an estimate of the actual behaviour of the rock. One can, however, use an empirical description of the dependence of strength on strain rate, temperature, effective confining pressure to estimate changes in rock deformation, i.e.,

$$d(\ln(\sigma) = \frac{\partial \ln(\sigma)}{\partial \ln(\dot{\varepsilon})}\bigg|_{P,\frac{1}{T}} d(\ln \dot{\varepsilon}) + \frac{\partial \ln(\sigma)}{\partial \ln(P)}\bigg|_{\dot{\varepsilon},\frac{1}{T}} d(\ln P) - \frac{\partial \ln(\sigma)}{\partial \ln(\frac{1}{T})}\bigg|_{P,\dot{\varepsilon}} \quad (4)$$

If equation 3 adequately describes the deformation, then the first term in equation (4) is 1/n, the second is zero, and the last is Q/nR. In the following, we cast these empirical coefficients in terms of apparent values of n and Q to estimate strength, while recognizing that a more complex constitutive law is necessary to describe behavior in the semi-brittle regime.

Using the equation 4 (with pressure variation exponent ≈ 0), to obtain the loading rate dependency, strain rate-steps and stress relaxations were applied in most runs and the stress exponent n was determined from linear least squares regression fit to the logarithm of stress versus to the logarithm of strain rate data at each temperature for a given sample. The activation energy was determined from a least squares fit to the logarithm stress at rate versus inverse absolute temperature data, or by correcting the strain rates to a given constant stress at each temperature and fitting the logarithm strain rate versus inverse temperature (Fig. 4).

For *GB* sample we used this equation (4), between 600°C and 900°C and at confining pressure of 300 MPa. For *GFB* sample we used this equation between 850°C and 950°C at a confining pressure of 300 MPa.

The results show that n decreases with increasing temperature. For the *GB*, n ranges from 3.2 to 4.6. For the *GFB*, n ranges from 2.9 to 4.2. Average values of n, *Q* and A were taken for *GB*, *GFB* respectively.

In terms of strength, stress exponent and deformation mechanisms, the activation energy was calculated. The results are as follows *GB*: $Q = 180$ kJ.mol^{-1} ± 10; *GFB*: $Q = 990 \pm 50$ kJ.mol^{-1}; with these results, constant A can be calculated by equation (1).

Then we have the steady state flow laws for each temperature region as follows:

$$\text{GB: } \varepsilon' = (10^{-4}).\sigma^{(4.0\pm 0.7)}.\exp((-(180 \pm 10))/RT)$$

$$\text{GFB: } \varepsilon' = (10^{30}).\sigma^{(3.5\pm 0.7)}.\exp((-(990 \pm 50))/RT)$$

The stress exponents and activation energies found for *GB* at temperature between 800 and 900°C° are similar to the ones found for a glassy basalt by Hacker and Christie, 1992.

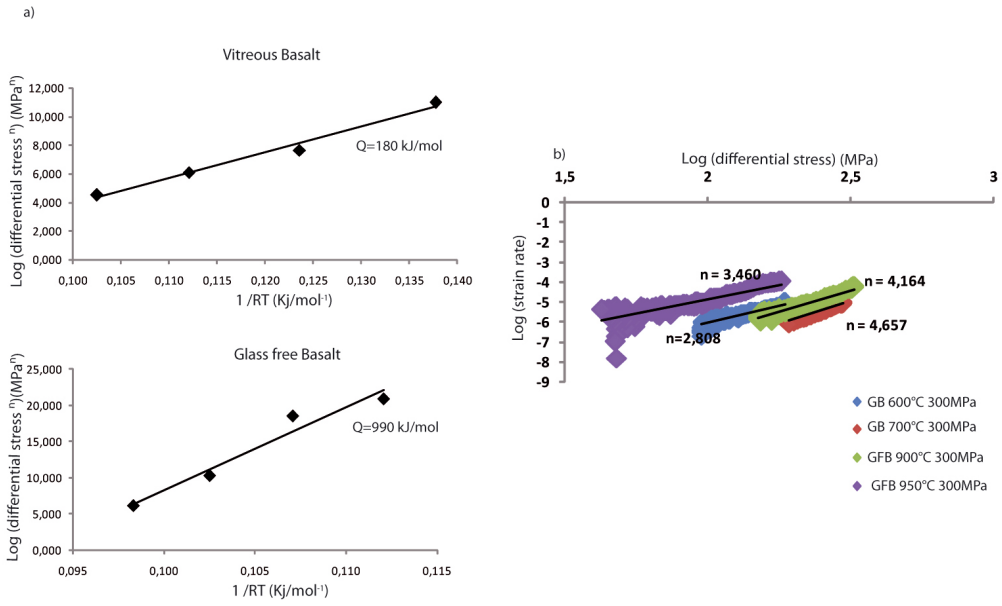

Figure 4: a) plots of stress versus temperature for the vitreous basalt and the glass free basalt. b) Several plots of log strain rate versus log stress for the sample GB at 600°C and 700°C at a confining pressure of 300 MPa and for the sample GFB 900°C and 950°C at a confining pressure of 300 MPa.

4.3. Rheological Profile

Rheological profiles in the case of a basaltic crust are plotted in the strength envelope in Figure 5 using strain rate of 10^{-14} and a thermal gradient of the Icelandic crust at the axial rift zone of 100°C /km (*Flóvenz and Sæmundsson, 1993; Bjornsson, 2008*). The friction law of *GB* and *GFB* and flow laws of *GB* and *GFB* determined above were used to calculate the resulting differential stress as a function of depth. All of the rheologies plotted in Figure 5 result from the extrapolation of our data to slower strain rate than those in the deformation experiments and on the assumption that rock at depth consists exclusively of basalt. The validity of the extrapolation is also strongly dependent on the accuracy of the determination of μ based on the friction law and on n and *Q* derived on the flow law. For *GB* sample the error on *Q* is ± 10 kJ/mol that corresponds to an error of ± 100 m in depth. For *GFB* sample the error on *Q* is ± 50 kJ/mol that corresponds to an error of ± 400 m on the depth of the brittle to ductile transition. The standard deviation of n ± 0.7 for *GB* and *GFB* causes on error of about 100 m on the depth of the brittle to ductile transition. Strength envelope shows that glassy basalt may deform in ductile regime at low temperature (about 200°C) whereas glass free basalt may deform in the brittle field up to 600°C-800°C.

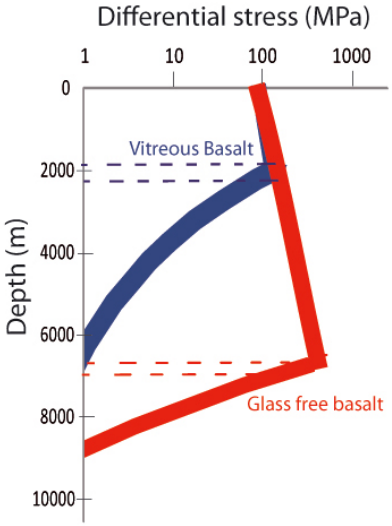

Figure 5: Differential stress versus depth for typical Iceland crust at the rift axis. Crustal temperature is calculated with a thermal gradient of about 100°C/km.

5. CONCLUSIONS: IMPLICATIONS FOR GEOTHERMAL EXPLOITATION

Mechanical observations at a constant strain rate of 1×10^{-5} s^{-1} and a confining pressure of 100 MPa and 300 MPa and extrapolation of mechanical results to geological strain rates indicate that basaltic rocks may deform in the brittle field to temperature up 600 to 800°C. Comparison with background temperature gradients close to the volcanic zone in Iceland (~100°C/km) indicate that, hydrothermal fluids might circulate, at least transiently, through the oceanic basaltic crust down to 6 to 8 km depth and supercritical fluids might be expected from 4 to 6 km depth within the volcanic rift zone (Fig. 5). These results are coherent with the lower limit of the Icelandic seismogenic zone which seems to be associated with a 750 ± 100°C isothermal surface (*Tryggvason, 2002; Ágústsson and Flovenz, 2005*).

It is important to note that our experiments were done only in the undrained condition for a limited set of strain rates and pressures. Because the rocks are deforming by both cataclastic and temperature dependent processes, the exact scaling of strength with effective lithostatic pressure, pore-fluid pressure, and deformation rate needs further clarification. When pore fluids are present, chemical and mechanical interactions with the rock matrix may cause important modifications to the geometry of the pore space that will undoubtedly influence both the rock strength and the fluid transport properties of the rocks. Such effects are likely to be profound and it will be important to investigate these for both engineering and scientific applications.

REFERENCES

Ágústsson, K., Flovenz, Ó.G., (2005). The Thickness of the Seismogenic Crust in Iceland and its Implications for Geothermal Systems. *WGC 2005 manuscript.*

Bjornsson, A. (2008). Temperature of the Icelandic crust: Inferred from electrical conductivity,temperature surface gradient, and maximum depth of earthquakes, *Tectonophysics*, v. 447, 136-141.

Escartin J., Andreani M., Hirth G., Evans B., (2008). Relationship between the microstructural evolution and rheology of talc at elevated pressure and temperature. *Earth & Planetary Science Letters, v. 268, 463–475.*

Flovenz, O.G., Saemundsson, K., (1993). Heat flow and geothermal processes in Iceland. *Tectonophysics*, v. 225, 123-138.

Fridleifsson G.O., Elders W.A., (2005). The Iceland Deep Drilling Project: a search for deep unconventional geothermal resources. *Geothermics*, v. 34, 269-285.

Hacker, B.R., Christie, J.M., (1992). Experimental deformation of a glassy basalt: *Tectonophysics*, v. 200, 79-96.

Macdonald K. C., (1982). “mid-ocean ridges" Fine Scale Tectonic, Volcanic and Hydrothermal Processes Within the Plate Boundary Zone Ann. *Rev. Earth Planet. Sci*. v. 10, 155-190.

Massiot C, Pezard P.A, Asmundsson R., *in prep* Achievements and ongoing progress of the European HiTI project: High Temperature Instruments for supercritical geothermal reservoir characterization and exploitation , *WGC 2010 manuscript*.

Palmason, G. and K. Sæmundsson, (1979). Iceland in relation to the Mid-Atlantic Ridge, Ann. Rev. Earth and Plan. Sci. Lett., v. 2, 25-50.

Paterson, M.S., (1978). Experimental Rock Deformation — The Brittle Field. *Springer-Verlag, Heidelberg-Berlin-New York, N.Y.*. 254 pp.

Rocchi, V., Sammonds, P.R. and Kilburn, C.R.J. (2003). Flow and fracture maps for basaltic rock deformation at high temperatures. *Journal of Volcanology and Geothermal Research, v.* 120. 25-42. ISSN 03770273

Tryggvason, A., S. Th. Rögnvaldsson, and Ó. G. Flóvenz, (2002). Three dimensional imaging of the P- and S-wave velocity structure and earthquake locations beneath southwest Iceland. Geophys. J. Int., V.151, 848-866, doi:10.1046/j.1365-246X.2002.01812.x.